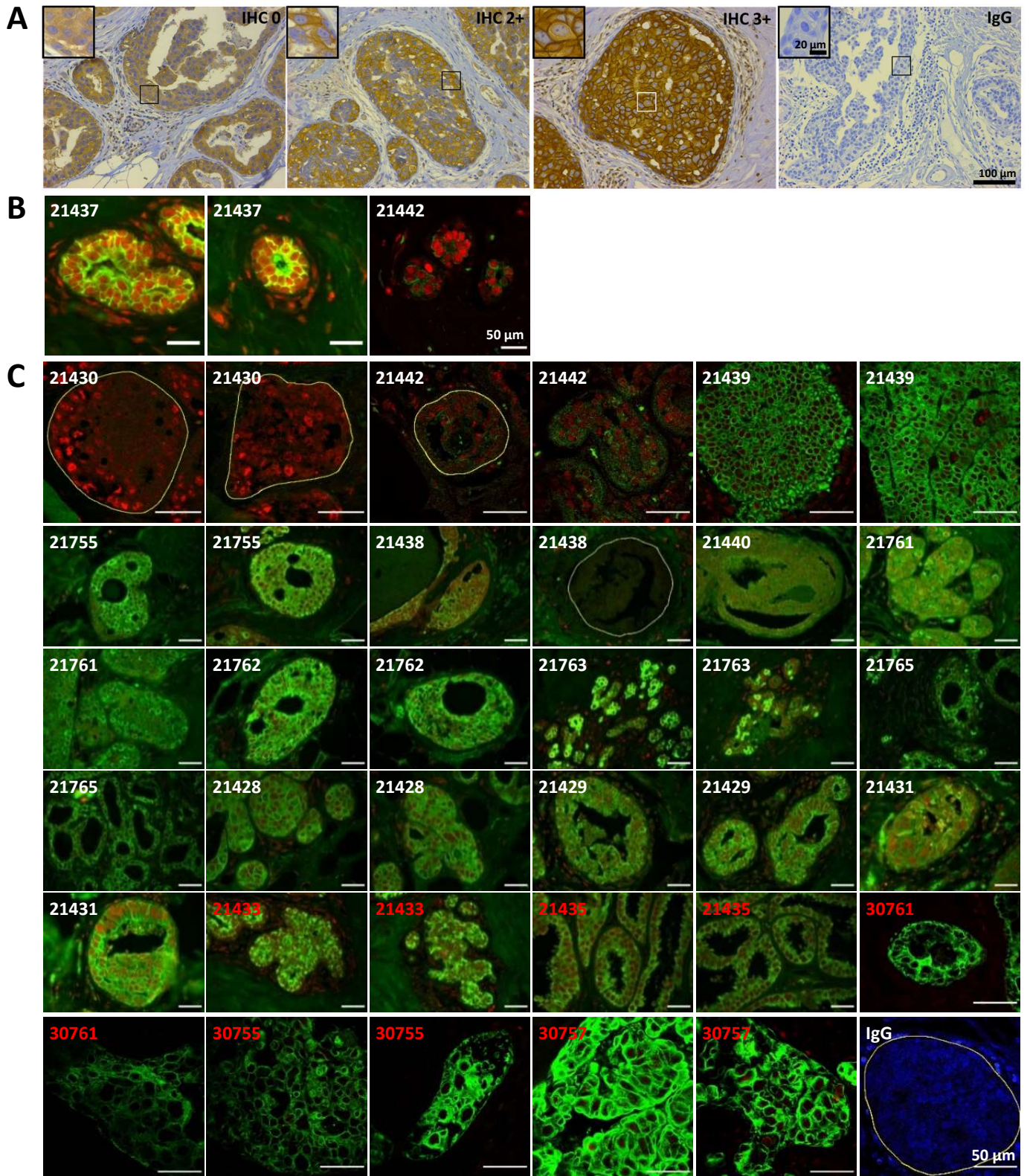
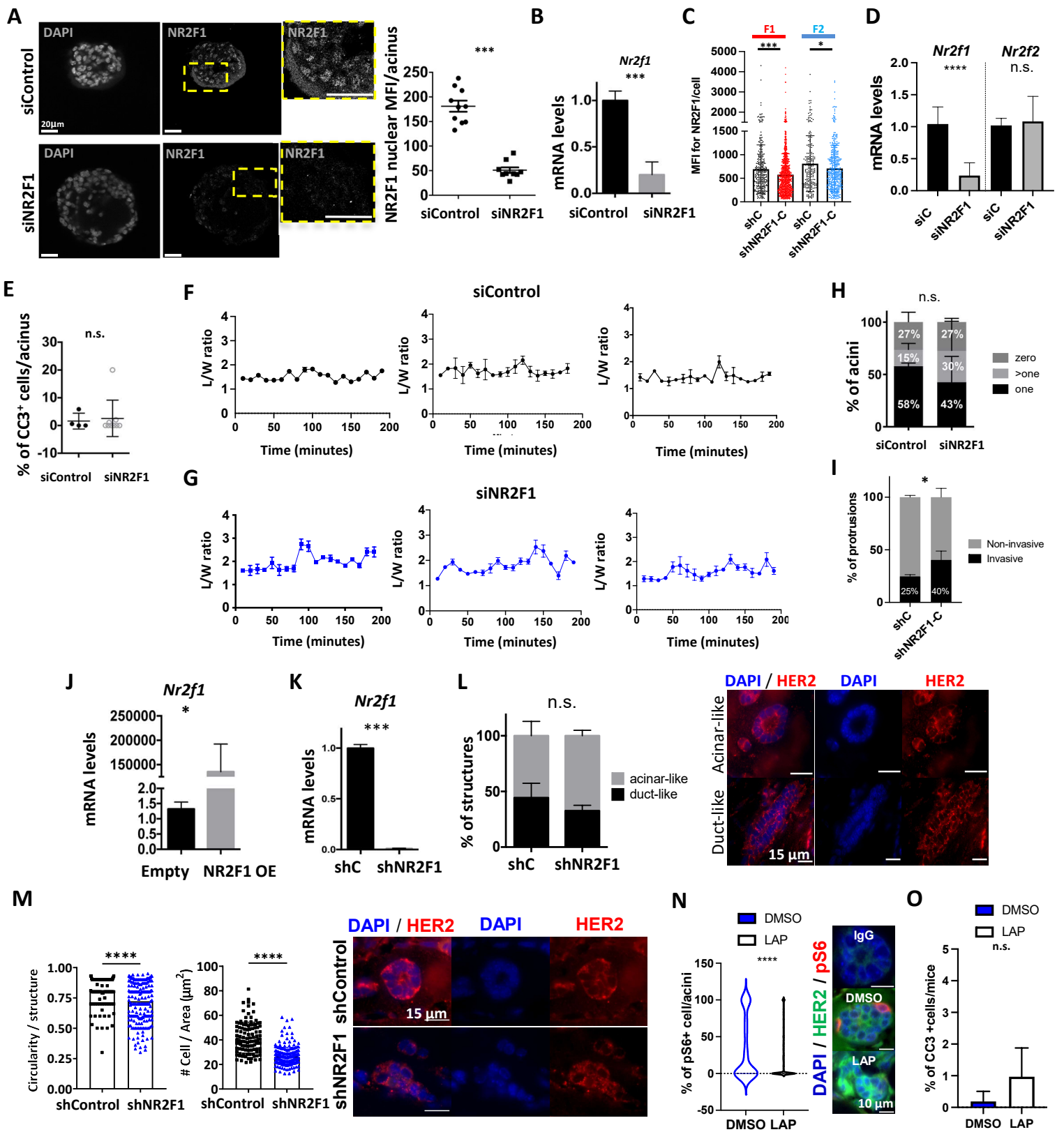


**Supplementary Figure 1. NR2F1 is downstream of HER2 and p38 signals.** **A.** QPCR for the indicated genes in MMTV-HER2 ECCs and treated with SB203580. N=2. **B.** WB for the indicated antigens from MMTV-HER2 ECCs in 2D (left). QPCR for *Nr2f1* and *Nr2f2* (right). N=2. **C.** WB for the indicated antigens from MDA-MB-361 and BT474 cells after treatment with WIP1 inhibitor (left). QPCR for *Nr2f1* and *Nr2f2* (right). N=2. **D.** Percentage of nuclear NR2F1 per duct by IHC in mammary glands from control or MKK3<sup>-/-</sup>/MKK6<sup>+/-</sup> mice. N=2 mice/group. Mann-Whitney test. **E.** QPCR for *Nr2f1* and *Nr2f2* in MMTV-HER2 ECCs grown in 2D after transfection with siRNAs **F.** Knockdown efficiency by QPCR for *Mapk14* (*p38alpha*) and *Mapk11* (*p38beta*) in MMTV-HER2 ECCs grown in 2D after transfection with siRNAs (left). WB for P38alpha, NR2F1, total P38, and Tubulin are shown to the left. N=2. Numbers show densitometry of NR2F1 bands in 2 independent experiments. **G.** QPCR for *Nr2f1* in sphere cultures from FvB-derived MECs treated with Lapatinib. N=3. **H.** QPCR for *Nr2f1* and WB for phospho-HER2 in SUM225 cells treated with Lapatinib. N=2. **I.** QPCR for the indicated genes in BT474 and MDA-MB-361 cells transfected with siHER2. N=3. **J.** Efficacy of SB203580, TAK715, and lapatinib treatments from **Fig. 1E.** WB for total ATF2 and p-ATF2 upon SB203580 or TAK715 treatment (left) and WB against pS6 upon lapatinib treatment (right) of MMTV-HER2 ECCs seeded in 2D. Numbers show densitometry of p-ATF2 bands in 2 independent experiments. **K.** QPCR for *NR2F1* and *NR2F2* from SUM225 cells treated with SB203580 or TAK715 (left and middle panels). QPCR for *NR2F1* in SUM225 cells incubated with SB203580 or TAK715 alone or in combination with lapatinib (right). For all graphs, mean±SD is shown and student's unpaired *t*-test, unless otherwise noted.

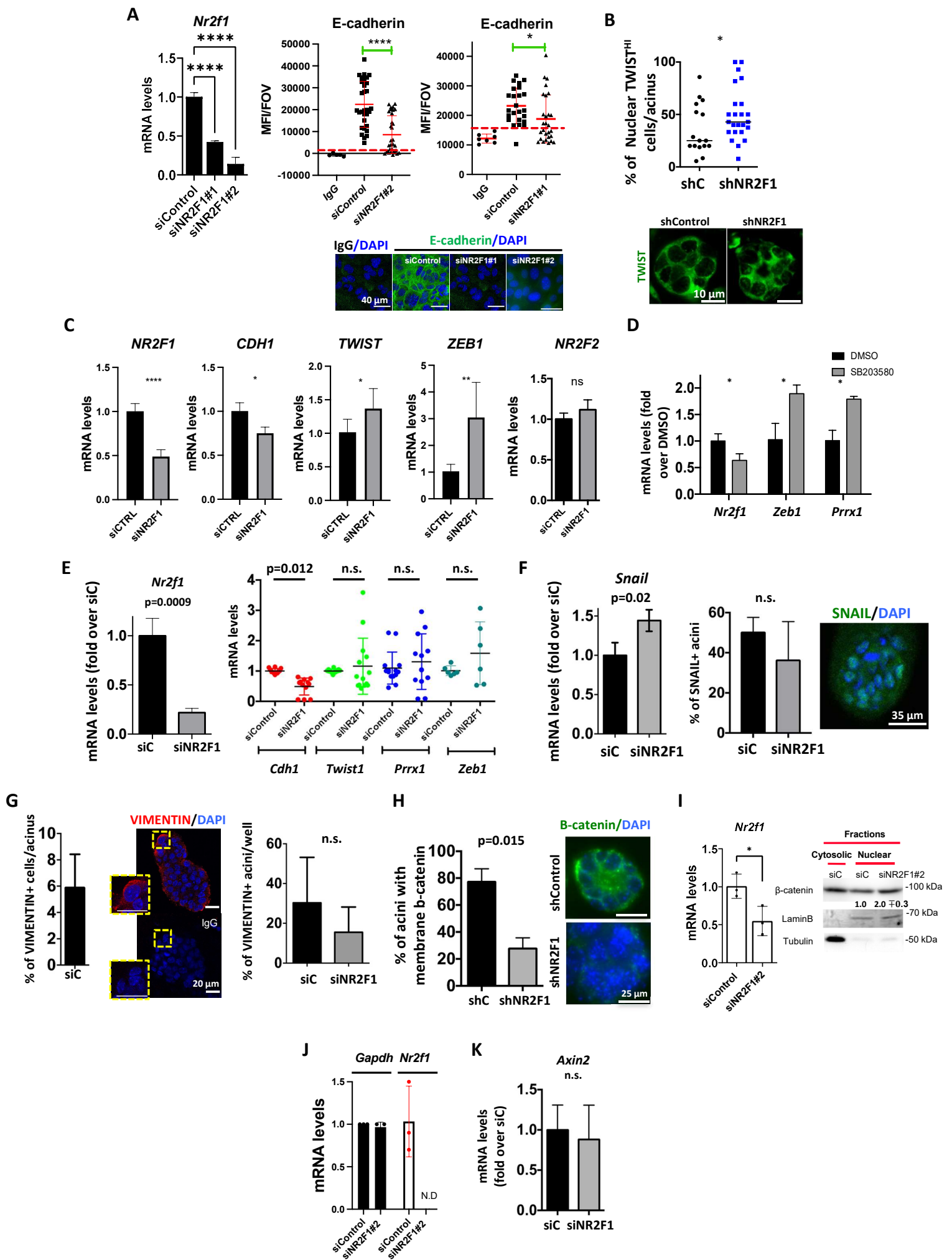


Rodriguez-Tirado et al. Supp Figure 2

**Supplementary Figure 2. HER2 scoring and NR2F1 staining in DCIS samples.** **A.** HER2 staining and scoring by IHC in DCIS samples (n=21). **B.** IF staining for NR2F1 (red) and Cytokeratin18 or panCytokeratin (Green) in benign adjacent areas in DCIS samples. **C.** IF staining for NR2F1 (red) and Cytokeratin18 or panCytokeratin (Green) in DCIS samples. DCIS areas with cytokeratin negative staining are delimited by a yellow line. HER2- (score 0-2+) and HER2+ (score 3+) patient status is marked by labels in white and red, respectively. For all, one or two representative images per patient are shown. IgG control shows DAPI staining (Blue).

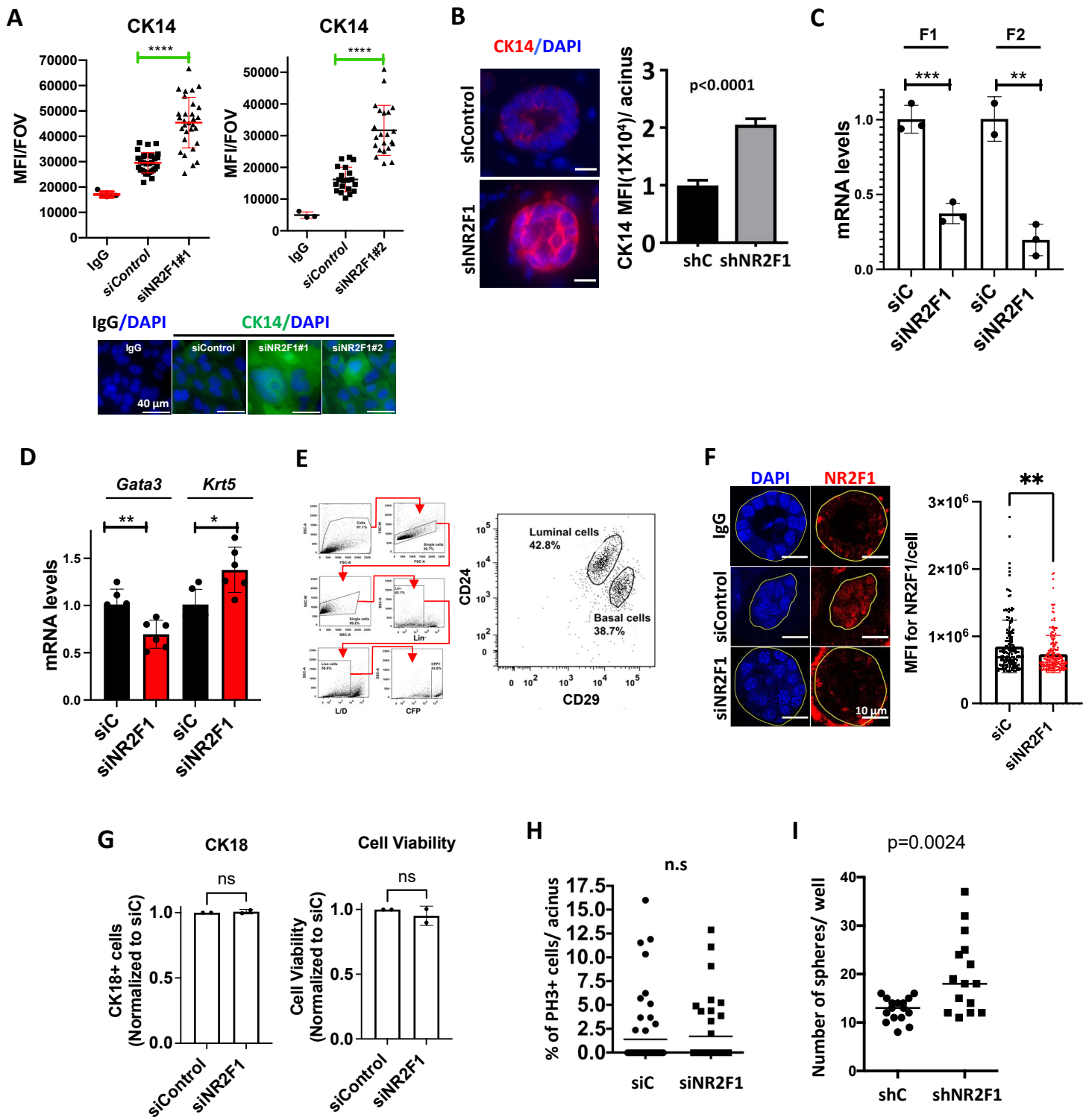


**Supplementary Figure 3. NR2F1 inhibits ECC invasion. A&B.** NR2F1 knockdown by IF (**A**) and QPCR (**B**) in acini from freshly isolated MMTV-HER2 ECCs after siRNA transfections. N=3. **C.** Knockdown efficiency by IF from MMTV-HER2 ECC acini after transduction with shRNA. N=2. **D.** QPCR for *Nr2f1* and *Nr2f2* from MMTV-HER2 ECCs grown in 2D after NR2F1 knockdown. N=3. **E.** Percentage of CC3+ MMTV-HER2 ECCs per acinus by IF after siRNA transfections. N=2. **F & G.** Representative L/W ratio of one protrusion/acini in siControl (**F**) or siNR2F1 (**G**) acini. **H.** Percentage of acini with zero, one or more than one protrusion after transfection with siRNA. N=2. Two-way ANOVA. **I.** Percentage invasive or non-invasive protrusions in acini from freshly isolated MMTV-HER2 ECCs after transduction with shRNA as described in C. N=2. Fisher's exact test. **J.** QPCR for *Nr2f1* in MMTV-HER2 ECCs after transfection with pcDNA-NR2F1 (OE) or control empty plasmid. **K.** QPCR for *Nr2f1* in stable shRNA MMTV-HER2 ECC organoid lines. **L.** Percentage of HER2+ acinar-like and duct-like structures in mammary glands of animals injected with shControl and shNR2F1 MMTV-HER2 ECCs described in K. N=3 animals/group. Two-way ANOVA. **M.** Circularity and cell density in acinar-like structures in mammary glands described in L. N=3 animals/group. Mann-Whitney. **N.** Percentage of pS6+ cells/acinus in mammary fat pad injected with shControl and shNR2F1 MMTV-HER2 ECCs and treated with lapatinib for 48 h before tissue collection. N=2-4 animals/group. **O.** Percentage of CC3+ cells in the mammary fat pad of animals described in L determined by IF. For all graphs, mean (dot plots) or mean±SD (bar graphs) is shown and student's unpaired *t*-test, unless otherwise noted.



**Supplementary Figure 4. NR2F1 depletion allows a partial EMT and hybrid luminal/basal program in ECCs.** **A.** E-cadherin expression in MMTV-HER2 ECCs grown in 2D after transfection with siRNAs. Knockdown validation by QPCR (left). **B.** Percentage of TWIST1+ cells per acinus in mammary glands injected with shControl and shNR2F1 MMTV-HER2 ECCs described in **Supp. Fig. 3K**. N=2 mice/group. **C.** QPCR for the indicated genes in SUM225 cells transfected with siRNAs for 48 h. N=2. **D.** QPCR for the indicated genes in acini from freshly isolated MMTV-HER2 ECCs treated with DMSO or SB203580 for 48 hours. N=2. **E.** QPCR for the indicated genes in acini from freshly isolated FvB-derived MECs after transfection with siRNAs. Knockdown validation by QPCR (left). N= 2-6. **F.** SNAIL expression levels by QPCR (left) and IF (right) in acini from freshly isolated MMTV-HER2 ECCs after NR2F1 knockdown. Percentage of SNAIL+ acini/well is shown. N=2. **G.** Percentage of Vimentin+ cells/acinus (left) or Vimentin+ acini/well (right) from freshly isolated MMTV-HER2 ECCs after NR2F1 knockdown. Representative image of the siControl group is shown. N=2. **H.** Percentage of  $\beta$ -catenin+ acini in mammary glands injected with shControl and shNR2F1 MMTV-HER2 ECCs described in **Supp. Figure 3K**. N=2 mice/group. **I.** WB for  $\beta$ -catenin in nuclear fractions of MMTV-HER2 ECCs after NR2F1 downregulation. Knockdown validation by QPCR (left). N=3. **J.** QPCR for *Nr2f1* in MMTV-HER2 ECCs grown in 2D after transfection with siNR2F1#2. N=2. N.D.=not determined. **K.** QPCR for *Axin2* in acini from freshly isolated MMTV-HER2 ECCs after NR2F1 knockdown. N=4. For all graphs, mean (dot plots) or mean $\pm$ SD (bar graphs) is shown and student's unpaired *t*-test performed.





**Supplementary Figure 5. NR2F1 depletion favors a hybrid luminal/basal phenotype and stemness capacity in ECCs.** **A.** CK14 expression in MMTV-HER2 ECCs grown in 2D after transfection with siRNAs. Knockdown validation by QPCR shown in **Supp. Fig. 4A**. **B.** CK14 expression in mammary glands injected with shControl and shNR2F1 MMTV-HER2 ECCs described in **Supp. Fig. 3K**. N=3 animals/group. **C&D.** QPCR for *Nr2f1* (**C**) *Gata3*, and *Krt 5* (**D**) in acini from freshly isolated MMTV-HER2 ECCs transfected with siRNAs. N=2. **E.** Gating strategy for FACS sorting of luminal MMTV-HER2 ECCs (live Lin-CFP+CD24<sup>Hi</sup>CD29+). **F.** NR2F1 knockdown validation by IF (MFI, mean fluorescence intensity/cell) from sorted luminal MMTV-HER2 ECCs transfected with siRNAs. Representative images of MMTV-HER2 acini stained with NR2F1 (red) are shown. **G.** CK18 expression and viability by FC from sorted luminal MMTV-HER2 ECCs grown in acini and transfected with siRNAs. N=2. **H.** Percentage of pH3+ cells in acini from freshly isolated MMTV-HER2 ECCs after NR2F1 knockdown. N=3. **I.** Sphere count for shControl and shNR2F1 MMTV-HER2 ECCs after 1 week. N=3. For all graphs, mean (dotplot) or mean±SD (bar graph) is shown and student's unpaired *t*-test performed.

**Movies 1&2-** Early cancer acini transfected with siControl were imaged for 4 hours every 10 min.

**Movies 3&4-** Early cancer acini transfected with siNR2F1 were imaged for 4 hours every 10 min.

**Movies 5-** shControl early cancer cells injected into the fat pad of nude mice were imaged for half an hour every 2 minutes by multiphoton microscopy. The movie is a representative region of one mouse.

**Movies 6-** shNR2F1 early cancer cells injected into the fat pad of nude mice were imaged for half an hour every 2 minutes using multiphoton microscopy. The movie is a representative region of one mouse.